Inorganic Chemistry

Article

pubs.acs.org/IC

Synthesis and Properties of New Phosphorescent Red Light-Excitable Platinum(II) and Palladium(II) Complexes with Schiff Bases for Oxygen Sensing and Triplet−Triplet Annihilation-Based Upconversion

Sergey M. Borisov,*[,†] Robert Saf,[‡] Roland Fischer,[§] and Ingo Klimant[†]

[†]Institute of Analytical Chemistry and Food Chemistry, [‡]Institute of Chemistry and Technology of Materials, and [§]Institute of Inorganic Chemistry, Graz University of Technology, Stremayrgasse 9, 8010, Graz, Austria

Supporting Information

ABSTRACT: New Pt(II) and Pd(II) complexes with donor−acceptor Schiff bases are conveniently prepared in only two steps. The complexes efficiently absorb in the red part of the spectrum ($\varepsilon > 10^5$ M^{-1} cm^{-1}) and show moderate to strong room-temperature phosphorescence in the near-infrared (NIR) region. Particularly, Pt(II) complexes possess phosphorescence quantum yields (Φ) of ∼10%, but the emission of the respective Pd(II) complexes is less efficient ($\Phi \approx 1\%-2\%$). The complexes exhibit solvatochromic behavior, in which the absorption and emission spectra shift bathochromically in polar solvents. The Pt(II) complexes are embedded in polystyrene to produce oxygen-sensing materials. The Pd(II) and Pt(II) complexes are demonstrated to be efficient sensitizers in triplet−triplet annihilation-based upconversion systems.

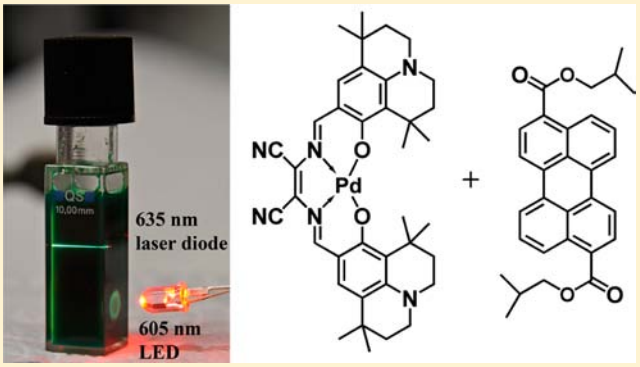

1. INTRODUCTION

Phosphorescent metal complexes receive much attention, because of their application in organic light-enmitting diodes (OLEDs),[1−3] photovoltaic devices,[4,5] optical sensors,[6,7] and probes and as luminescent labels,[8] which are particularly useful for imaging applications in biology.[9,10] Red-light- and NIR-excitable complexes are particularly promising for sensing and labeling applications, because they have much lower levels of autofluorescence (compared to the established UV−vis dyes) and lower light scattering, and because of their potential for measurements in tissues and living organisms ("smart tattoos").[11−13] Because of the singlet oxygen that is produced upon quenching, some complexes also find application in photodynamic therapy.[14] Furthermore, these chromophores were applied in near-infrared (NIR) organic light-emitting diodes (OLEDs).[15−17] In the last couple of years, such complexes became interesting as sensitizers in triplet−triplet annihilation (TTA)-based upconversion systems,[18−20] primary because of the potential application of such systems in photovoltaics. Considering application in TTA-upconversion systems, red-light-excitable sensitizers are also of particular interest, since the maximum flux of sunlight peaks occurs at ∼680 nm.[21] However, most of the sensitizers applied so far in such systems absorb in the blue and green parts of the spectrum.[22−30] Red excitation is rare, and the sensitizers used are mostly represented by complexes of benzoporphyrins and phthalocyanines.[31−36] Recently reported sensitizers based on iodinated BODIPY dyes[37] and BODIPYs bound to Pt(II) complexes[38] represent a notable exception.

Currently, red-light-excitable phosphorescent dyes are limited to heavy-metal complexes of porphyrins and their analogues, including π-extended benzoporphyrins,[39−41] naphthoporphyrins[42−44] and their hybrids,[45] phthalocyanines,[46] azabenzoporphyrins,[47] chlorins,[48] corrols,[49] etc. The above-mentioned new multichromophoric systems based on BODIPY-Pt(II) complex hybrids were also found to be phosphorescent in the NIR region.[38] Evidently, new NIR-emitting complexes based on chromophores other than porphyrins and their analogues would be very interesting, since such dyes may possess photophysical properties that differ substantially from the known compounds. Recently, Che and co-workers reported photophysical properties of platinum(II) complexes with Schiff bases and their applications in OLEDs.[50,51] These green-emitting complexes were found to be strongly phosphorescent (quantum yields (Φ) up to 27%). On the other hand, the molar absorption coefficients in the blue part of the spectrum are below 10 000 M^{-1} cm^{-1}, which is rather low to achieve sufficient brightness in sensing materials. Wu et al. demonstrated enhancement of the absorption for some of the Pt(II) Schiff base complexes and their application in the TTA-based upconversion system.[27] On the other hand, Schiff bases

Received: July 3, 2012
Published: December 11, 2012

containing both donor and acceptor substituents are known to possess bathochromically shifted absorption spectra and are highly fluorescent ($\Phi \approx 80\%$).[52,53] The zinc complex is also highly fluorescent[53] and was recently demonstrated to have a rather high two-photon absorption cross-section (up to 200 GM).[54] Evidently, the combination of these long-wavelength-excitable ligands with platinum group metals may result in a new class of phosphorescent NIR dyes. In this contribution, we report on the preparation and characterization of novel red-light excitable phosphorescent dyes based on platinum(II) and palladium(II) complexes with donor−acceptor Schiff bases and demonstrate the application of the former as oxygen indicators. We will also demonstrate the potential of the new dyes as sensitizers in TTA-based upconversion systems.

2. EXPERIMENTAL SECTION

Materials. Diaminomaleonitrile, 4-diethylamino-2-hydroxybenzaldehyde, 1,1,7,7-tetramethyl-8-hydroxy-9-formyljulolidine, diphenylether, benzonitrile, potassium carbonate, and methansulfonic acid were obtained from Aldrich. Platinum(II) chloride and palladium(II) chloride, diisobutyl 3,9-perylenedicarboxylate were obtained from ABCR (Karlsruhe, Germany); silica gel, polystyrene (MW 250000), and all other solvents were obtained from Acros (Wien, Austria). Poly(ethylene glycol terephthalate) support (Mylar) was obtained from Goodfellow (Oakdale, PA, USA). Sulforhodamine 101 was purchased from Radiant Dyes (Wermelskirchen, Germany); *N*,*N*′-bis-(2,6-diisopropylphenyl)-1,6,7,12-tetra-(4-phenoxy)perylene-3,4,9,10-tetracarboxylic acid diimide (Lumogen F Red), *N*,*N*′-bis-(2,6-diisopropylphenyl)-perylene-3,4,9,10-tetracarboxylic acid diimide (Lumogen F Orange) were obtained from Kremer Pigmente GmbH and Co. KG (Aichstetten, Germany); and 3-dibutylaminophenol was obtained from TCI Europe. Nitrogen, oxygen, synthetic air, and argon (all of 99.999% purity) were obtained from Linde (Graz, Austria).

Platinum(II) and palladium(II) bis(benzonitrile)dichlorides ($Pt(C_6H_5CN)_2Cl_2$ and $Pd(C_6H_5CN)_2Cl_2$, respectively) were obtained by dissolving platinum(II) and palladium(II) chlorides, respectively, in hot benzonitrile and precipitating the complex with hexane. Platinum(II) tetraphenyltetrabenzoporphyrin (PtTPTBP) was prepared according to the literature procedure.[16,41] The preparation of the 4-dibutylamino-2-hydroxybenzaldehyde from 3-dibutylaminophenol is reported elsewhere.[55]

Synthesis. *2,3-Bis[(4-diethylamino-2-hydroxybenzylidene)-amino]but-2-enedinitrile (**1**).* A modified literature procedure was used.[56] 4-Diethylamino-2-hydroxybenzaldehyde (1.546 g (8 mmol)) and 415 mg (3.84 mmol) of diaminomaleonitrile were dissolved in 250 mL of ethanol, and 150 μL of methansulfonic acid was added as a catalyst. The solution was stirred for 6 h at 40 °C. The dark green sediment was isolated by filtration and washed three times with methanol. The product was purified on a silica-gel column, using dichloromethane as an eluent. Yield: 1.2 g (68%) of dark green crystals. MS (MALDI): *m*/*z* $[M]^+$ 458.2430 calc., 458.2442 found. ^{1}H NMR (300 MHz, $CDCl_3$), ppm: 12.89 (s, 2H; OH), 8.49 (s, 2H; HC═N), 7.20 (d, 2H; Ph), 6.33 (d, 2H; Ph), 6.30 (s, 2H; Ph), 3.44 (q, 8H; CH_2), 1.23 (t, 12H; CH_3). ^{13}C NMR (75 MHz, $CDCl_3$), ppm: 12.7, 45.2, 98.1, 106.0, 109.8, 112.6, 121.9, 135.6, 153.7, 161.9, 164.4.

*Platinum(II) 2,3-bis[(4-diethylamino-2-hydroxybenzylidene)-amino]but-2-enedinitrile (**Pt-1**).* 183 mg (0.4 mmol) of **1** and 200 mg (0.42 mmol) of $Pt(C_6H_5CN)_2Cl_2$ were dissolved in 60 mL of diphenylether and the solution was stirred at 200 °C for 2 h. Then, 200 mg (1.45 mmol) of potassium carbonate and 200 mg of $Pt(C_6H_5CN)_2Cl_2$ were added. The solution was stirred overnight at 200 °C. The UV−vis spectroscopy indicated almost full conversion of the ligand to the Pt(II) complex. The reaction mixture was cooled to room temperature and 200 mL of dichloromethane were added. The metallic platinum was separated by centrifugation and the complex was precipitated with hexane. The operation was repeated twice to remove diphenylether. The complex was purified on a silica-gel column using dichloromethane as an eluent. Yield: 90 mg (35%) of golden crystals. MS (MALDI): *m*/*z* $[M]^+$ 650.1901 calc., 650.1911 found. ^{1}H NMR (300 MHz, $CDCl_3$), ppm: 8.03 (s, 2H; HC═N), 7.32 (d, 2H; Ph), 6.61 (s, 2H; Ph), 6.43 (d, 2H; Ph), 3.47 (q, 8H; CH_2), 1.27 (t, 12H; CH_3). ^{13}C NMR spectrum was not acquired, because of the low solubility of the complex. Analysis for $C_{26}H_{28}N_6O_2Pt$: found C 47.89, H 4.30, N 12.71. Calc. C 47.92, H 4.33, N 12.90.

*Palladium(II) 2,3-bis[(4-diethylamino-2-hydroxybenzylidene)-amino]but-2-enedinitrile (**Pd-1**).* 183 mg (0.4 mmol) of **1** and 240 mg (0.62 mmol) of $Pd(C_6H_5CN)_2Cl_2$ were dissolved in 100 mL of diphenylether, and the solution was stirred at 180 °C for 1.5 h. The solution was cooled to RT and 200 mL of dichloromethane were added. The metallic palladium was separated by centrifugation and the complex was precipitated with hexane. The operation was repeated twice to remove diphenylether. The complex was purified on a silica-gel column using dichloromethane as an eluent. Yield: 140 mg (62%) of golden crystals. MS (MALDI): *m*/*z* $[M]^+$ 562.1319 calc., 562.1387 found. ^{1}H NMR (300 MHz, $CDCl_3$), ppm: 7.72 (s, 2H; HC═N), 7.17 (d, 2H; Ph), 6.48 (s, 2H; Ph), 6.35 (d, 2H; Ph), 3.45 (q, 8H; CH_2), 1.25 (t, 12H; CH_3). ^{13}C NMR spectrum was not acquired due to the low solubility of the complex. Analysis for $C_{26}H_{28}N_6O_2Pd$: Found: C 55.31, H 4.89, N 14.69. Calc.: C 55.47, H 5.01, N 14.93.

*2,3-Bis[(4-dibutylamino-2-hydroxybenzylidene)amino]but-2-enedinitrile (**2**).* 4-Dibutylamino-2-hydroxybenzaldehyde (550 mg (2.2 mmol)) and 108 mg (1 mmol) of diaminomaleonitrile were dissolved in 30 mL of ethanol, and 40 μL of methansulfonic acid was added as a catalyst. The solution was stirred for 6 h at 40 °C. The dark green sediment was isolated by filtration and washed three times with methanol. The product was purified on a silica-gel column using the mixture of toluene and dichloromethane (1:1) as an eluent. Yield: 420 mg (74%) of black crystals. MS (MALDI): *m*/*z* $[M]^+$ 570.3682 calc., 570.3646 found. ^{1}H NMR (300 MHz, $CDCl_3$), ppm: 12.29 (s, 2H; OH), 8.49 (s, 2H; HC═N), 7.17 (d, 2H; Ph), 6.31 (d, 2H; Ph), 6.18 (s, 2H; Ph), 3.34 (t, 8H; $\underline{CH_2}$-CH_2−CH_2−CH_3), 1.62 (p, 8H; CH_2−$\underline{CH_2}$−CH_2−CH_3), 1.38 (sex, 8H; CH_2−CH_2−$\underline{CH_2}$−CH_3), 0.97 (t, 12H; CH_3). ^{13}C NMR (75 MHz, $CDCl_3$), ppm: 13.9, 20.3, 29.5, 51.3, 98.1, 106.0, 109.6, 111.3, 125.9, 135.1, 153.7, 161.4, 163.8.

*Platinum(II) 2,3-bis[(4-dibutylamino-2-hydroxybenzylidene)-amino]but-2-enedinitrile (**Pt-2**).* 143 mg (0.25 mmol) of **2** and 160 mg (0.34 mmol) of $Pt(C_6H_5CN)_2Cl_2$ were dissolved in 40 mL of diphenylether and the solution was stirred at 160 °C for 2h. During the reaction nitrogen was bubbled through the solution. Then, 40 mg (0.09 mmol) of $Pt(C_6H_5CN)_2Cl_2$ were added and the stirring was continued for another 2 h. The UV−vis spectroscopy indicated almost full conversion of the ligand to the Pt(II) complex. The reaction mixture was cooled to room temperature and the product was precipitated with hexane. The complex was purified on a silica-gel column using a toluene:dichloromethane (1:1) mixture as an eluent. Yield: 66 mg (35%). MS (MALDI): *m*/*z* $[M]^+$ 762.3152 calc., 762.3194 found. ^{1}H NMR (300 MHz, $CDCl_3$), ppm: 7.94 (s, 2H; HC═N), 7.21 (d, 2H; Ph), 6.56 (d, 2H; Ph), 6.38 (s, 2H; Ph), 3.37 (t, 8H; $\underline{CH_2}$−CH_2−CH_2−CH_3), 1.67 (p, 8H; CH_2−$\underline{CH_2}$−CH_2−CH_3), 1.39 (sex, 8H; CH_2−CH_2−$\underline{CH_2}$−CH_3), 0.99 (t, 12H; CH_3). ^{13}C NMR (75 MHz, $CDCl_3$), ppm: 13.9, 20.3, 29.8, 51.3, 100.4, 108.4, 111.2, 115.1, 121.6, 136.4, 146.2, 155.0, 167.9. Analysis for $C_{34}H_{44}N_6O_2Pt$: found C 53.47, H 5.66, N 10.99. Calc. C 53.46, H 5.81, N 11.00.

*Palladium(II) 2,3-bis[(4-dibutylamino-2-hydroxybenzylidene)-amino]but-2-enedinitrile (**Pd-2**).* 228 mg (0.4 mmol) of **2** and 230 mg (0.6 mmol) of $Pd(C_6H_5CN)_2Cl_2$ were dissolved in 60 mL of diphenylether and the solution was stirred at 150 °C for 3 h. During the reaction, nitrogen was bubbled through the solution. The reaction mixture was cooled to room temperature and the product was precipitated with hexane. The complex was purified on a silica-gel column using a toluene:dichloromethane (1:1) mixture as an eluent. Yield: 100 mg (37%). MS (MALDI): *m*/*z* $[M]^+$ 672.2567 calc., 672.2603 found. ^{1}H NMR (300 MHz, $CDCl_3$), ppm: 7.68 (s, 2H; HC═N), 7.12 (d, 2H; Ph), 6.44 (d, 2H; Ph), 6.33 (s, 2H; Ph), 3.35 (t, 8H; $\underline{CH_2}$−CH_2−CH_2−CH_3), 1.64 (p, 8H; CH_2−$\underline{CH_2}$−CH_2−CH_3), 1.38 (sex, 8H; CH_2−CH_2−$\underline{CH_2}$−CH_3), 0.98 (t, 12H; CH_3). ^{13}C NMR (75 MHz, $CDCl_3$), ppm: 13.9, 20.3, 29.8, 51.3, 100.0, 107.9,

dx.doi.org/10.1021/ic301440k | *Inorg. Chem.* 2013, 52, 1206−1216

Scheme 1. Synthetic Procedures for the Ligands and Metal Complexes

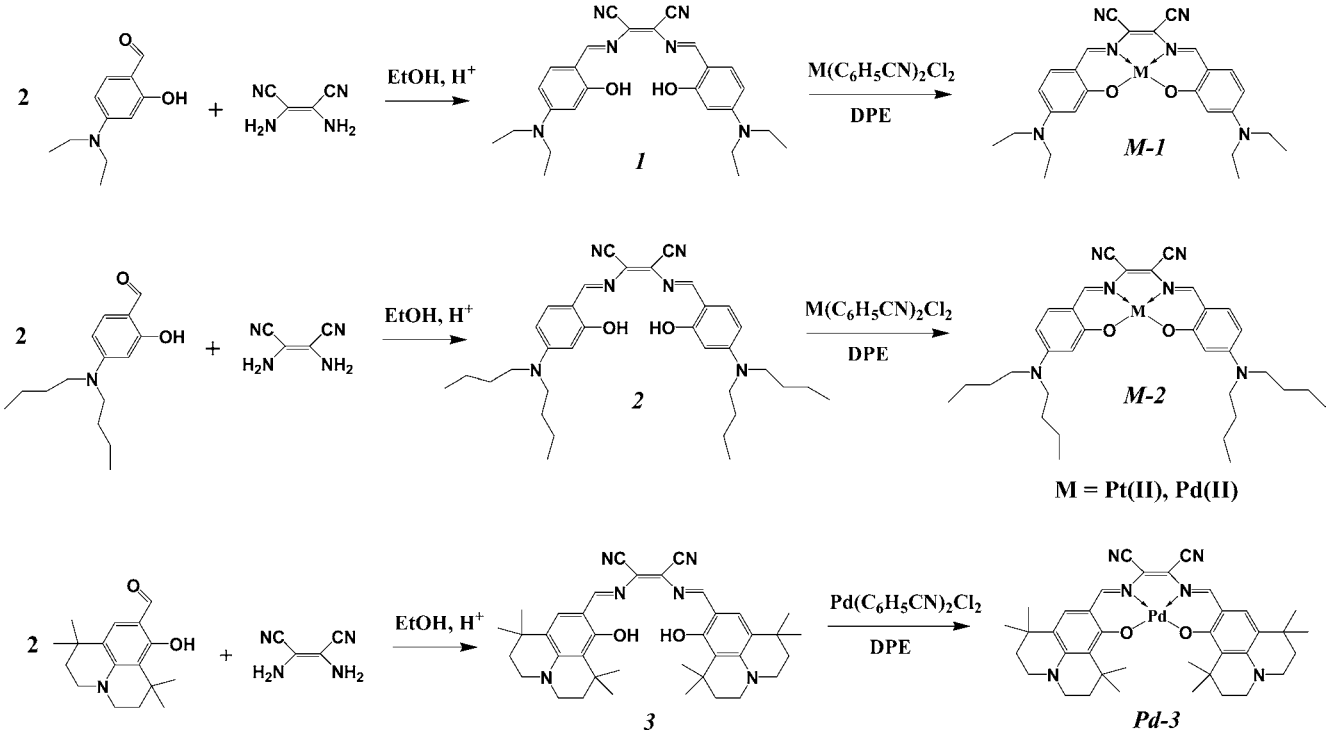

110.6, 114.6, 119.5, 136.7, 148.6, 155.4, 168.9. Analysis for $C_{34}H_{44}N_6O_2Pd$: Found: C 60.36, H 6.30, N 12.43. Calc.: C 60.48, H 6.57, N 12.45.

*2,3-Bis(3,3,9,9-tetramethyl-2-hydroxyjulolidine)but-2-enedinitrile (**3**).* 1,1,7,7-Tetramethyl-8-hydroxy-9-formyljulolidine (1.094 g (4 mmol)) and 210 mg (1.94 mmol) of diaminomaleonitrile were dissolved in 50 mL of ethanol, and 100 μL of methansulfonic acid were added. The solution was stirred for 6 h at 40 °C. The solvent was evaporated under vacuum, and the product was purified on a silica-gel column using dichloromethane as an eluent. Yield: 770 mg (64%) of dark green crystals. MS (MALDI): m/z $[M]^+$ 618.3682 calc., 618.3657 found. ^{1}H NMR (300 MHz, $CDCl_3$), ppm: 13.43 (s, 2H; OH), 8.40 (s, 2H; HC═N), 6.99 (s, 2H; Ph), 3.36 (t, 4H; CH_2N), 3.26 (t, 4H; CH_2N), 1.75 (m, 8H; CH_2), 1.53 (s, 12H; CH_3), 1.27 (s, 12H; CH_3). ^{13}C NMR (75 MHz, $CDCl_3$), ppm: 28.0, 30.2, 31.7, 32.2, 35.7, 39.5, 47.3, 47.8, 109.7, 113.0, 114.2, 120.8, 124.5, 129.3, 148.8, 161.3.

*Palladium(II) 2,3-bis(3,3,9,9-tetramethyl-2-hydroxyjulolidine)but-2-enedinitrile (**Pd-3**).* 170 mg (0.275 mmol) of **3** and 211 mg (0.55 mmol) of $Pd(C_6H_5CN)_2Cl_2$ were dissolved in 60 mL of diphenylether. The solution was stirred at 180 °C for 1.5 h. The solution was cooled to room temperature, and 150 mL of hexane were added. The mixture was brought on the silica-gel column and eluted with hexane, a hexane:toluene (1:1) mixture, and toluene to remove the ligand and the side products. The complex was eluted with a toluene:dichloromethane (1:1) mixture and recrystallized from dichloromethane:ethanol to give golden crystals. Yield: 30 mg (15%) of golden crystals. MS (MALDI): m/z $[M]^+$ 722.2575 calc., 722.2516 found. ^{1}H NMR (300 MHz, $CDCl_3$), ppm: 7.72 (s, 2H; HC═N), 6.97 (s, 2H; Ph), 3.39 (t, 4H; CH_2N), 3.28 (t, 4H; CH_2N), 1.76 (m, 8H; CH_2), 1.60 (s, 12H; CH_3), 1.29 (s, 12H; CH_3). ^{13}C NMR (75 MHz, $CDCl_3$), ppm: 28.1, 29.7, 31.9, 33.0, 35.7, 39.9, 47.4, 47.9, 111.3, 114.7, 115.0, 118.1, 126.3, 129.4, 147.4, 150.2, 166.3. Analysis for $C_{38}H_{44}N_6O_2Pd{\cdot}0.5CH_2Cl_2$: Found: C 60.31, H 5.72, N 10.87. Calc.: C 60.39, H 5.92, N 10.98.

Preparation of the Oxygen Sensors. Two milligrams (2 mg) of a Pt(II) complex and 400 mg of polystyrene were dissolved in 8 g of chloroform. The solution was knife-coated on the Mylar support to give a sensing film ~5 μm thick after evaporation of the solvent.

Measurements. ^{1}H and ^{13}C NMR spectra were recorded on a Bruker Avance III 300 MHz Spectrometer at 300 and 75 MHz, respectively. MALDI-TOF mass spectra were recorded on a Micromass TofSpec 2E. The instrument is equipped with a nitrogen laser (337 nm wavelength, operated at a frequency of 5 Hz), and a time lag focusing unit. Spectra were taken in reflectron mode at an accelerating voltage of +20 kV. *Trans*-2-[3-(4-*tert*-butylphenyl)-2-methyl-2-propenylidene]malononitrile (DCTB) and dithranol were used as matrix. Analysis of data was done with MassLynx 3.4 (Micromass, Manchester, U.K.). Absorption spectra were measured at a Cary 50 UV−vis spectrophotometer (Varian). Emission spectra were acquired on a Hitachi Model F-7000 fluorescence spectrometer (Japan) equipped with a red-sensitive photomultiplier R 9876 from Hamamatsu (Japan). The solutions were degassed by passing argon through the sealable quartz cuvette from Hellma (Müllheim, Germany) for 15 min. All the spectra were corrected for the sensitivity of the photomultiplier. Luminescence quantum yields of the Schiff base ligands were determined relative to Sulforhodamine 101 (Φ = 0.95 in ethanol)[57] and Lumogen F Red (Φ = 0.96 in chloroform).[58] Luminescence quantum yields of the complexes were determined relative to PtTPTBP (Φ = 0.51 in toluene).[41] Luminescence spectra at 77 K were acquired on a Fluorolog 3 fluorescence spectrometer from Horiba (Japan) equipped with a NIR-sensitive photomultiplier R2658 from Hamamatsu (Japan) optimized for the spectral range of 300−1050 nm. The dyes were dissolved in a mixture of toluene and tetrahydrofuran (4:6 v/v), which was found to produce good glass at 77 K. The relative luminescence quantum yields were estimated using Lumogen F Red as a standard and assuming Φ = 1 in toluene/tetrahydrofuran glass at 77 K.

Luminescence decay times were measured with a two-phase lock-in amplifier (Model SR830, Stanford Research Inc., USA) equipped with a photomultiplier tube (H5701-02, Hamamatsu, Japan). A 590-nm LED and a 605-nm LED (both from Roithner Lasertechnik, Austria) were used for the excitation of solutions and sensor foils, respectively. The light of the LEDs was filtered through a NIR-blocking Calflex X filter (Linos) and the long-pass RG 9 filter was used for the emission. A bifurcated fiber bundle was used to guide the excitation light to samples and the emission light back to the photomultiplier. The modulation frequencies were 5 kHz and 20 kHz for the palladium(II) and platinum(II) complexes, respectively. Three independent

dx.doi.org/10.1021/ic301440k | *Inorg. Chem.* 2013, 52, 1206−1216

measurements were performed. Temperature was controlled using a cryostat ThermoHaake DC50 (Thermo Fisher Scientific, Inc.).

The triplet−triplet annihilation upconversion experiments were performed in toluene solutions which were thoroughly deoxygenated with argon. The red laser diode module (LJM Series, λ_{max} 635, Roithner Lasertechnik) was used for the excitation. The emission spectra of the upconverted fluorescence were acquired on a Fluorolog 3 fluorescence spectrometer. Neutral density filters from Lee Filters were used to obtain the dependence of the intensity of the upconverted fluorescence on photon flux density. The photon flux density was determined with a Li-250A light meter from Li-COR (Lincoln, NE, USA).

Photobleaching experiments were performed with solutions of the dyes in dimethylformamide in a 1-cm glass cuvette. A 3-W 590-nm LED was used for excitation (photon flux = 3.6×10^{20} ph s^{-1} m^{-2}). The cuvette was shaken every 60 s to provide sufficient oxygen supply. Photobleaching of the sensors was investigated using the same setup as that used to determine the luminescence decay times.

Crystal Structure Determination. A crystal of **Pd-3** of ∼0.79 mm × 0.46 mm × 0.11 mm was mounted on the tip of a glass fiber. Data for **Pd-3** were collected at 100 K on a Bruker KAPPA8 APEXII instrument with use of Mo Kα (λ = 0.71073 Å) radiation and a CCD area detector. The SHELX version 6.1 program package was used for the structure solutions and refinements.[59] Absorption corrections were applied using the SADABS program.[60] The crystal structures were solved by direct methods and refined by full-matrix least-squares procedures. In one of the crystallographically distinct molecules of **Pd-3** one of the annellated cyclohexylamine units in the ligand periphery is found disordered over two positions. The disorder was fully refined using the part instruction, site occupancies refined to 51% vs 49%. Despite the disorder, all non-hydrogen atoms were refined anisotropically. All hydrogen atoms were included in the refinement at calculated positions using a riding model, as implemented in the SHELXTL program.

3. RESULTS AND DISCUSSION

Synthesis. The platinum(II) and palladium(II) complexes with donor−acceptor Schiff bases can be conveniently prepared in only two steps (Scheme 1). The ligands **1** and **3** are synthesized in high yields from commercially available 2-hydroxybenzaldehydes and diaminomaleonitrile. The ligand **2** is prepared analogously to **1** and **3** using a 4-dibutylamino-2-hydroxybenzaldehyde instead. The second step involves metallation of the ligands with platinum(II) or palladium(II) bis(benzonitrile) dichloride in diphenylether (DPE), according to the procedure reported previously for benzoporphyrins.[61] Similarly to the metallation of porphyrins, the Pd(II) complexes are formed more readily than the respective Pt(II) complexes where higher temperatures, longer reaction times or the addition of base (K_2CO_3) are necessary. We found that bubbling of nitrogen through the heated solution can facilitate the metalation both for palladium and platinum since the hydrochloric acid formed is removed. In this case, the addition of the potassium carbonate is not necessary. The metallation of **3** is more challenging, and, unfortunately, we were not able to isolate the Pt(II) complex with ligand **3** in analytically pure form. Nevertheless, the synthesis of all other complexes is favorably compared to the multistep preparation of the π-extended porphyrins,[40] and this can be an important factor for practical applications.

X-ray Crystal Structure. **Pd-3** crystallizes in the triclinic space group $P\bar{1}$ with two independent molecules of the Pd(II) Schiff-base complex in the asymmetric unit, together with one additional molecule of the solvent methylene chloride.

In both crystallographically independent units of **Pd-3**, the palladium(II) center adopts a strictly square planar, 4-fold coordinated environment with sums of X−Pd−X angles (X = O, N, respectively) of 359.99(10)° and 359.98(10)° (Figure 1).

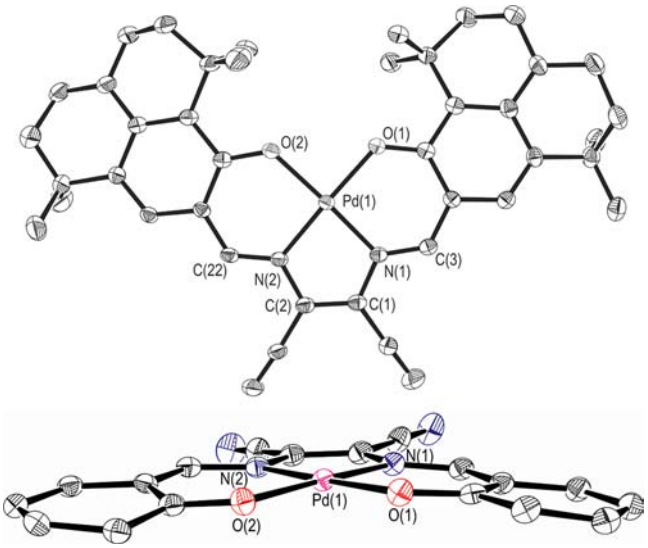

Figure 1. Thermal ellipsoid plot of **Pd-3** at 50% probability level. Selected bond distances and angles are as follows: Pd(1)−O(1), 1.977(2) (1.986(2)) Å; Pd(1)−O(2), 1.9815(19) (1.982(2)) Å; Pd(1)−N(1), 1.953(2) (1.952(2)) Å; Pd(1)−N(2), 1.948(2) (1.951(2)) Å; C(1)−C(2), 1.379(4) (1.373(4)) Å; C(1)−N(1), 1.384(4) (1.398(4)) Å; C(2)−N(2), 1.388(3) (1.398(4)) Å; N(1)−C(3), 1.331(3) (1.322(4)) Å; N(2)−C(22), 1.331(3) (1.315(4)) Å; ∠N(1)−Pd(1)−N(2), 83.9(9)° (84.22(10)°), ∠O(1)−Pd(1)−N(1), 93.73(9)° (93.50(9)°); ∠O(2)−Pd(1)−N(2), 93.97(9)° (93.36(9)°); and ∠O(1)−Pd(1)−O(2), 88.35(8)° (88.94(8)°). (Note that protons and the second independent molecule **Pd-3**(2) are not shown, for the sake of clarity; numbers shown in parentheses indicate the bond distances and angles for **Pd-3**(2).)

Among these, the N−Pd−N angles are smallest at ∼84°. The O−Pd−O angles adopt values at ∼88° and the largest values are observed for the O−Pd−N angles. These deviations from 90° are caused by the rigid ligand backbone.

The Pd−N distances fall in a range between 1.948(2) Å and 1.953(2) Å. For the Pd−O bond lengths, values between 1.977(2) Å and 1.986(2) Å are found. The N−C distances of the imino-groups in the ligand backbone account for relatively short values (between 1.315(4) Å and 1.331(3) Å). The central C−C atoms are separated by only 1.379(4) Å and 1.373(4) Å. The variation of bond distances in the ligand suggests only a limited delocalization of electron density along the C−N backbone of the substituent. The two independent Pd centers are separated by 10.664(4) Å in the crystal (11.294(4) and 13.656(4) Å for Pd2−Pd2A and Pd1−Pd1A, respectively). Thus, a direct electronic interaction of the metallo-centers is ruled out. Crystal data and structure refinement for **Pd-3** are summarized in Table 1.

Photophysical Properties. Absorption and emission spectra of the Schiff bases and the respective metal complexes are shown in Figure 2. As can be observed, **3** and its Pd(II) complex absorb and emit at longer wavelengths than **1** and **2**. This can be explained by the higher electron-donating ability of the more-rigid julolidine, compared to the dialkylamino group. In fact, a similar trend is observed for other dye classes, such as coumarins, rhodamines, etc. (e.g., λ_{max} = 470 and 478 nm for 3-(2-benzothiazolyl)-7-(diethylamino)coumarin (Coumarin 6) and 10-(2-benzothiazolyl)-2,3,6,7-tetrahydro-1,1,7,7-tetrameth-

dx.doi.org/10.1021/ic301440k | Inorg. Chem. 2013, 52, 1206−1216

Table 1. Crystal Data and Structure Refinement for Pd-3

parameter	value/comment
empirical formula	$C_{38}H_{44}N_6O_2Pd{\cdot}0.5CH_2Cl_2$
formula weight	765.66
temperature	100(2) K
wavelength	0.71073 Å
crystal system	triclinic
space group	$P\bar{1}$
unit-cell dimensions	
a	13.3376(4) Å
b	15.5220(5) Å
c	19.6685(7) Å
α	69.299(2)°
β	84.4650(10)°
γ	71.3980(10)°
volume, V	3609.4(2) Å^3
Z	4
density (calculated)	1.409 Mg/m^3
absorption coefficient	0.631 mm^{-1}
F(000)	1588
crystal size	0.79 mm × 0.46 mm × 0.11 mm
theta range for data collection	2.12°−30.00°
index ranges	$-17 \le h \le 18$, $-21 \le k \le 21$, $-27 \le l \le 26$
reflections collected	73282
independent reflections	20936 [R(int) = 0.0280]
completeness to theta = 30.00°	99.4%
absorption correction	SADABS
max. and min transmission	0.9367 and 0.6353
refinement method	Full-matrix least-squares on F^2
data/restraints/parameters	20936/0/948
goodness-of-fit on F^2	1.123
final R indices [$I > 2\sigma(I)$]	$R1$ = 0.0431, $wR2$ = 0.0947
R indices (all data)	$R1$ = 0.0721, $wR2$ = 0.1192
largest diff. peak and hole	2.072 and −1.986 e Å^{-3}

yl-1H,5H,11H-(1)benzopyropyrano(6,7−8-*i,j*)quinolizin-11-one, respectively, or 545 and 565 nm for Rhodamine B and Rhodamine 101, respectively). The bathochromic shift of the absorption and the emission with increasing of the electron-donating ability of NR_2 group in such push−pull chromophores is attributed to the increase of the HOMO energy in respect to that of the LUMO.[62] Although all the ligands show good solubility in the organic solvents the solubility of the complexes of **1** is limited and they tend to aggregate at concentration exceeding 5−7 × 10^{-3} M. However, the solubility greatly improves for the complexes of **2** and **3**.

The absorption and the emission spectra shift bathochromically upon metalation. Interestingly, palladium affects the absorption to a lower extent that platinum but the emission maxima for both Pd(II) and Pt(II) complexes are similar. Molar absorption coefficients are rather high and exceed 110 000 M^{-1} cm^{-1} for all the complexes (Table 2) and are comparable to the ε values obtained for the ligands. Thus, the new complexes not only absorb at 50−100 nm longer wavelength than the reported Pt(II) Schiff base complexes[37,51] but also possess significantly higher molar absorption coefficients in the visible (Vis) region. In fact, most of the reported dyes have a value of $\varepsilon \approx 10\,000$ M^{-1} cm^{-1} but was as high as 65 000 M^{-1} cm^{-1} for one of the complexes bearing diethylamino groups.[37]

The Pt(II) complexes show fairly strong NIR phosphorescence at room temperature (Figure 2). Evidently, the intersystem crossing is very efficient, because virtually no fluorescence from the coordinated ligand is observed. The phosphorescence quantum yields (Φ) are ∼10% (see Table 2). However, this value is much lower than those for the respective metal-free Schiff bases, which are very strong emitters ($\Phi \approx$ 90%). This indicates rather efficient radiativeless deactivation of the triplet state in the complexes. The quantum yields for the new Pt(II) complexes are ∼2-fold lower than that for the Pt(II) Schiff base complexes reported by Che and co-workers[51] and Zhao and co-workers.[37] This is in good agreement with significantly lower energy of the triplet state of the new dyes. As can be seen (Table 2), the Pd(II) complexes are rather poor emitters with $\Phi \approx$ 1%−2%. As expected, the luminescence decay times of the Pd(II) complexes are longer that those for the Pt(II) complexes (45−70 and 11−13 μs, respectively). Generally, the complexes of **2** possess slightly higher luminescence quantum yields and longer decay times compared to the complexes of **1**. For the Pt(II) and Pd(II) complexes, the luminescence excitation spectra (see Figure S1 in the Supporting Information) are virtually identical to the absorption spectra.

Phosphorescence spectra at 77 K (Figure S2 in the Supporting Information) are rather similar to those obtained in solution at room temperature. Both the luminescence quantum yields and the decay times increase at low temperature (see Table 2). The radiative rate constants ($k_r = \Phi/\tau$) are mostly similar at both temperatures but the nonradiative rate constants ($k_{nr} = (1 - \Phi)/\tau$) are significantly higher at room temperature. As can be observed, the increase of the luminescence quantum yields and the decay times at 77 K is more pronounced for the weaker-emitting Pd(II) complexes than for the Pt(II) dyes.

Comparison of the photophysical properties of the Schiff base complexes with those of the Pt(II) and Pd(II) *meso*-tetraphenyltetrabenzoporphyrins (TPTBP) shows that the position of the absorption and emission bands is very similar for both chromophore classes (see Table 2, as well as Figure S3 in the Supporting Information). Despite similarly high molar absorption coefficients, the absorption bands are much broader in case of the Schiff base complexes. In fact, the full width at half-maximum (fwhm) is ∼38 nm for the Pt(II)-Schiff base complexes and only 18 nm for the benzoporphyrin complexes. Because of this fact, the new complexes can be efficiently excited with a broad range of light-emitting diodes (LEDs), e.g., 590, 605, or 625 nm LED. Compared to PtTPTBP (see Figure S3 in the Supporting Information), the new complexes in equimolar concentration can collect about twice as much light in the region of 500−700 nm. The collection efficiency is even more impressive since the molecular weight of **Pt-2** is ∼25% lower than that of PtTPTBP. This places the new dyes among the most-efficient sensitizers for the green−red region and makes them particularly interesting for application in light conversion systems. Regarding the luminescence properties, the phosphorescence quantum yields of the Pt(II) benzoporphyrins are significantly higher and the decay times longer than for the Pt(II) Schiff base complexes.

Solvatochromic Behavior. Pronounced solvatochromic behavior could be expected due to the push−pull character of the Schiff base chromophores. Therefore, the effect of the

dx.doi.org/10.1021/ic301440k | Inorg. Chem. 2013, 52, 1206−1216

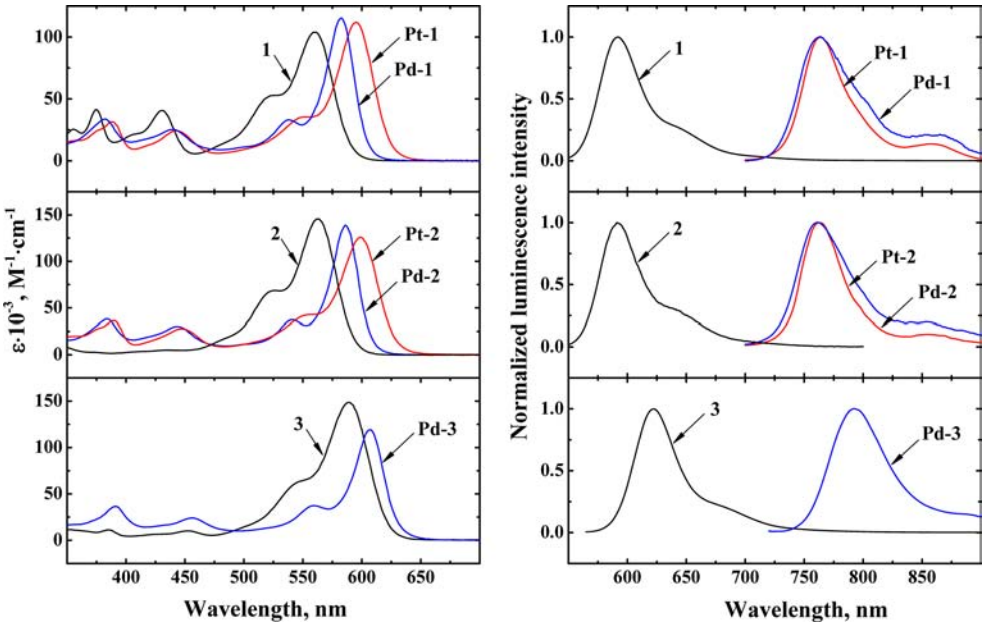

Figure 2. Absorption (left) and corrected emission spectra (right) of the Pd(II) and Pt(II) Schiff base complexes and the respective ligands.

Table 2. Photophysical Properties of the Schiff Bases and the Respective Platinum(II) and Palladium(II) Complexes in Toluene Solution at Room Temperature and in Toluene:Tetrahydrofuran (4:6 v/v) Glass at 77 K

	Room Temperature				77 K			
dye	λ_{max}abs ($\varepsilon \times 10^{-3}$)	λ_{max}em, nm	Φ, %	τ, μs	λ_{max} em, nm	E_T, cm^{-1}	Φ, %	τ, μs
1	375 nm (41 M^{-1} cm^{-1}); 431 nm (40 M^{-1} cm^{-1}); 525 nm (53 M^{-1} cm^{-1}); 560 nm (104 M^{-1} cm^{-1})	592	93	n.d.	n.d.	n.d.	n.d.	n.d.
Pt-1	389 nm (31 M^{-1} cm^{-1}); 443 nm (24 M^{-1} cm^{-1}); 552 nm (35 M^{-1} cm^{-1}); 596 nm (112 M^{-1} cm^{-1})	764	9.5	11	763	13100	11	19
Pd-1	383 nm (33 M^{-1} cm^{-1}); 439 nm (25 M^{-1} cm^{-1}); 538 nm (33 M^{-1} cm^{-1}); 583 nm (115 M^{-1} cm^{-1})	763	1.2	45	749	13400	5	180
2	526 nm (69 M^{-1} cm^{-1});; 563 nm (146 M^{-1} cm^{-1})	593	96	n.d.	n.d.	n.d.	n.d.	n.d.
Pt-2	390 nm (36 M^{-1} cm^{-1}); 447 nm (28 M^{-1} cm^{-1}); 555 nm (40 M^{-1} cm^{-1}); 599 nm (126 M^{-1} cm^{-1})	763	11	13	756	13200	13	19
Pd-2	384 nm (38 M^{-1} cm^{-1}); 444 nm (30 M^{-1} cm^{-1}); 541 nm (37 M^{-1} cm^{-1}); 586 nm (139 M^{-1} cm^{-1})	762	2.3	70	751	13300	3	180
3	386 nm (16 M^{-1} cm^{-1}); 452 nm (14 M^{-1} cm^{-1}); 550 nm (64 M^{-1} cm^{-1}); 589 nm (148 M^{-1} cm^{-1})	622	86	n.d.	n.d.	n.d.	n.d.	n.d.
Pd-3	391 nm (37 M^{-1} cm^{-1}); 455 nm (24 M^{-1} cm^{-1}); 560 nm (38 M^{-1} cm^{-1}); 607 nm (119 M^{-1} cm^{-1})	792	1.6	57	783	12800	4	130
PtTPTBP[a]	430 nm (205 M^{-1} cm^{-1}); 564 nm (16 M^{-1} cm^{-1}); 614 nm (136 M^{-1} cm^{-1})	770	51	47	760[b]	13200[b]	n.d.	59[b]
PdTPTBP[a]	443 nm (416 M^{-1} cm^{-1}); 578 nm (21 M^{-1} cm^{-1}); 628 nm (173 M^{-1} cm^{-1})	800	21	286	792[b]	12600[b]	n.d.	430[b]

[a]Data taken from ref 41. [b]Toluene glass at 77 K.

solvent polarity on the spectral properties of the complexes was investigated in detail. As an example, Figure 3 shows the absorption and the emission spectra of **Pt-2**. Similarly to the respective ligands, the polarity of the solvent affects the position of the absorption bands and the molar absorption coefficients. A more distinct dependency is observed for the emission spectra, which shift bathochromically with increasing polarity. In fact, a bathochromic shift of 50 nm (810 cm^{-1}) is observed upon going from hexane to dimethylsulfoxide (DMSO). The luminescence quantum yields decrease in polar solvents but also in a very apolar hexane (probably due to aggregation) and are ~5.8%, 11%, 8.5%, 7%, 4.8%, and 3.9% in hexane, toluene, chloroform, tetrahydrofuran (THF), acetonitrile, and DMSO, respectively. The decay times were determined to be 7.7, 13, 11.6, 9.6, 9.9, and 8.4 μs, respectively, in the same solvents. As can be seen (Figure S4 in the Supporting Information), similar solvatochromic behavior is observed for the corresponding ligand (**2**), but the bathochromic shift in the emission is even more significant (78 nm (2130 cm^{-1}) upon going from hexane to DMSO). Notably, the ligand possesses very efficient fluorescence in all the solvents (Φ = 55%, 96%, 94%, 90%, 86%, and 64% in hexane, toluene, chloroform, THF, acetonitrile, and DMSO, respectively). The solvatochromic behavior of **1** and **3** is similar to that of **2**. These properties make the metal-free dyes promising as long-wavelength excitable probes for monitoring solvent polarity.

Application in Optical Oxygen Sensors. The luminescence of all the complexes was found to be efficiently quenched by oxygen in solutions. This enables their application in optical oxygen sensors. Since the Pd(II) complexes show significantly lower luminescence brightness, only the sensors based on Pt(II) complexes were prepared and characterized. In

dx.doi.org/10.1021/ic301440k | Inorg. Chem. 2013, 52, 1206−1216

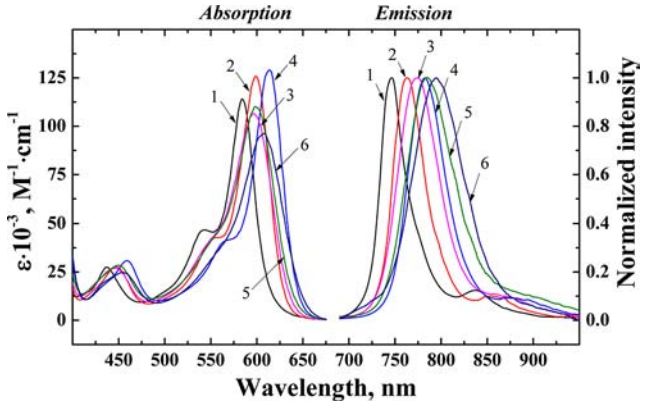

Figure 3. Absorption and emission spectra of **Pt-2** in hexane (spectrum 1), toluene (spectrum 2), tetrahydrofuran (THF) (spectrum 3), chloroform (spectrum 4), acetonitrile (spectrum 5), and dimethylsulfoxide (DMSO) (spectrum 6).

polystyrene, the absorption and the emission bands are bathochromically shifted, despite similar polarities of toluene and polystyrene (see Figures S5 and S6 in the Supporting Information, as well as Table 3). Figure 4 demonstrates the decay time and the Stern–Volmer plots for **Pt-1** embedded in polystyrene. Figure S7 in the Supporting Information shows the data for **Pt-2**. Similar to other oxygen indicators, the new complexes are prone to thermal quenching, which affects the luminescence decay time in the absence of the quencher (Table 3). The Stern–Volmer plots were fitted using an equation adapted from the "two-site model", which assumes localization of the indicator in two different environments:[63]

$$\frac{I}{I_0} = \frac{\tau}{\tau_0} = \frac{f_1}{1 + K_{SV}^1[O_2]} + \frac{f_2}{1 + K_{SV}^2[O_2]} \quad (1)$$

where f_1 and f_2 are the fractions of the total emission for each respective environment ($f_1 + f_2 = 1$), and K_{SV}^1 and K_{SV}^2 are the Stern–Volmer constants for each component. The relation $K_{SV}^2 = 0.1K_{SV}^1$ was used for fitting. As expected from the luminescence decay times, the K_{SV} values for the Pt(II) Schiff base complexes are lower than for the corresponding Pt(II) benzoporphyrins. On the other hand, the bimolecular quenching constants ($k_q = K_{SV}/\tau$) are similar for the Pt(II) Schiff bases and Pt(II) benzoporphyrins. Generally, although the oxygen sensors based on **Pt-1** and **Pt-2** show lower luminescence brightness than those based on Pt(II) benzoporphyrins, they can be promising for some applications where the cost of the indicator can be a concern (e.g., in food packaging).

Hai and co-workers[54] have recently demonstrated that Zn(II) complexes with donor–acceptor Schiff bases possess rather efficient 2-photon absorption cross sections (up to 200 GM). It can be expected that the Pt(II) complexes have similar nonlinear optical properties. Therefore, the new indicators may

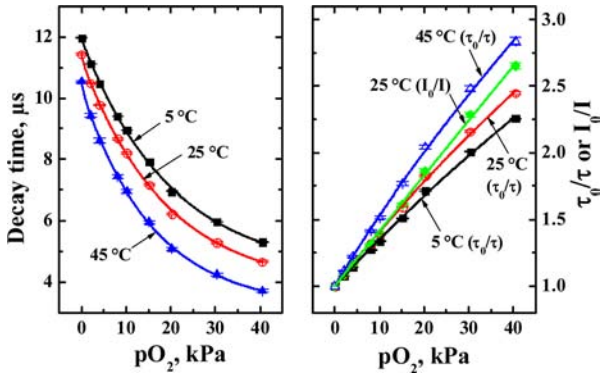

Figure 4. Response of the sensor based on **Pt-1** in polystyrene to oxygen: (left) decay time plots and (right) Stern–Volmer plots.

be promising for 2-photon imaging of oxygen in tissues, similar to the probes reported by Vinogradov and co-workers.[64,65]

Photostability. Photodegradation of the dyes was tested in air-saturated dimethylformamide (DMF) solutions where photobleaching is rather fast and, therefore, is easily measurable. It should be mentioned that photobleaching in most other commonly used solvents (e.g., toluene) is much slower. Generally, the long-wavelength absorption band disappears upon photobleaching but the absorption in the blue part of the spectrum slightly increases (see Figure S8 in the Supporting Information). Figure 5 and Figure S9 in the

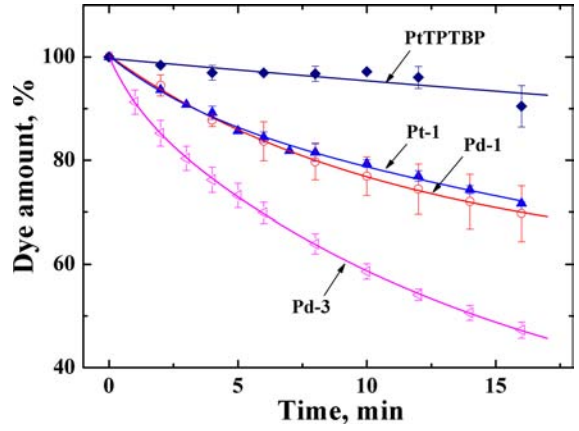

Figure 5. Photodegradation profiles of the Pt(II) and Pd(II) Schiff base complexes as well as PtTPTBP in DMF at 25 °C upon irradiation with a 590-nm high-power LED.

Supporting Information show photodegradation profiles of the Pt(II) and Pd(II) complexes with Schiff bases and Pt(II) *meso*-tetraphenyltetrabenzoporphyrin, which was used for comparison. As can be seen, the complexes with **2** and **3** bleach faster than with **1**. This may correlate with higher electron-donating character of the dibutylamino and julolidine groups, compared to the diethylamino group. However, in DMF, we did not

Table 3. Properties of the Polystyrene Optodes Based on the Platinum(II) Complexes

				K_{SV} (τ_0)				
indicator	λ_{max}abs, nm	λ_{max}em, nm	f_1	5 °C	25 °C	45 °C	$\Delta\tau_0$/K, %	ref
Pt-1	394, 453, 562, 606	767	0.85	0.043 kPa^{-1} (12.0 μs)	0.05 kPa^{-1} (11.4 μs)	0.065 kPa^{-1} (10.5 μs)	0.31	this work
Pt-2	393, 453, 564, 605	768	0.70	0.065 kPa^{-1} (11.5 μs)	0.077 kPa^{-1} (11.1 μs)	0.089 kPa^{-1} (10.7 μs)	0.18	this work
PtTPTBP	432, 566, 615	772	0.87		0.165 kPa^{-1} (55.3 μs)		0.06	66

dx.doi.org/10.1021/ic301440k | *Inorg. Chem.* 2013, 52, 1206–1216

observe a significant improvement in the photostability of the dyes upon deoxygenation with argon. It can also be concluded that the metal complexes of the donor–acceptor Schiff bases are less photostable than the platinum(II) porphyrin (see Figure 5).

Figure 6 and Figure S10 in the Supporting Information show photodegradation profile for the oxygen-sensing materials

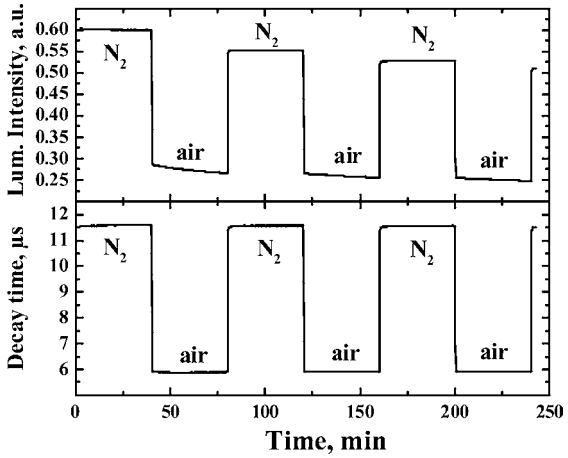

Figure 6. Photodegradation of **Pt-1** in polystyrene upon interrogation with a 20-mW 605-nm LED.

based on **Pt-1** in polystyrene and **Pt-2** in polystyrene, respectively. The sensors were continuously interrogated with a 605-nm LED. No bleaching is detectable under deoxygenated conditions, but some deterioration of the intensity (~2.7%/h) is observed under air saturation. This indicates that oxidation of the dyes with photosensitized singlet oxygen is the predominant photodegradation passageway in optical sensing materials based on the Pt(II) Schiff base complexes. Importantly, no drift in the luminescence decay time is observed, even at air saturation; therefore, no recalibration is necessary. It should be mentioned here that continuous interrogation is generally not required and a pulse of 100 ms is more than sufficient to obtain one measurement point (m.p.). Therefore, 1 h of continuous irradiation equals 100 h of measurements with the acquisition rate of 6 m.p./min, and photostability may not be critical for many applications.

Application in Triplet–Triplet Annihilation-Based Upconversion Systems. As was mentioned previously, triplet–triplet annihilation-based upconversion systems have been recently intensively investigated, because of their potential application in photovoltaics. Such systems rely on two main components: a sensitizer and an annihilator (see Figure S11 in the Supporting Information). Briefly, light absorption results in population of the triplet excited state of the sensitizer; the triplets of the annihilator are produced as a result of the triplet–triplet energy transfer. Finally, annihilation of the two excited annihilator molecules generates the sensitizer in the singlet excited state, which emits anti-Stokes fluorescence:

$$\mathbf{S}(S_0) + h\nu_1 \rightarrow \mathbf{S}(S_1)$$

$$\mathbf{S}(S_1) \rightarrow \mathbf{S}(T_1)$$

$$\mathbf{S}(T_1) + \mathbf{A}(S_0) \rightarrow \mathbf{S}(S_0) + \mathbf{A}(T_1)$$

$$\mathbf{A}(T_1) + \mathbf{A}(T_1) \rightarrow \mathbf{A}(S_1) + \mathbf{A}(S_0)$$

$$\mathbf{A}(S_1) \rightarrow \mathbf{A}(S_0) + h\nu_2$$

where **S** and **A** are the sensitizer and the annihilator, respectively. Importantly, very high molar absorption coefficients of the new dyes in the orange–red part of the spectrum and broad absorption bands make the new dyes particularly interesting for TTA-based upconversion. As a model system, we used a 1×10^{-4} M solution of the sensitizer and a 5×10^{-4} M solution of the annihilator in toluene. Perylene-based annihilators were employed (Figure 7) since they feature strong

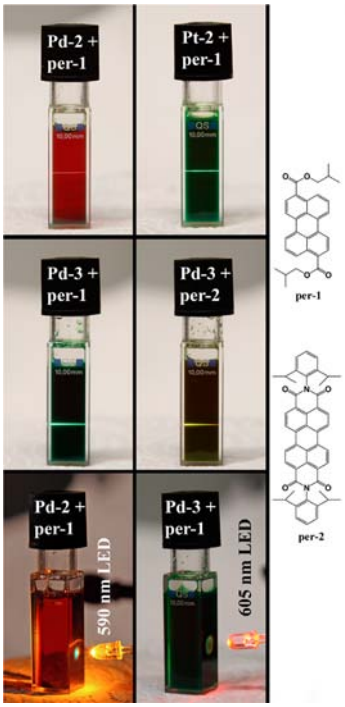

Figure 7. Photographic images of the solutions composed of 1×10^{-4} M of the sensitizer and 5×10^{-4} M of the annihilator in deoxygenated toluene upon excitation with a 635-nm laser diode, as well as with 5-mm LEDs. Chemical structures of the annihilators are also shown.

fluorescence with quantum yields approaching unity and their spectral properties can be varied by choosing an appropriate dye. As can be seen (Figure 7), the new dyes indeed act as efficient sensitizers of the upconverted fluorescence. Strong green fluorescence of diisobutyl 3,9-perylenedicarboxylate (**per-1**) is clearly visible upon excitation of the solutions containing **Pt-1**, **Pt-2**, and **Pd-3** with a 635-nm laser diode. The Pd(II) complexes of **1** and **2** absorb at shorter wavelengths so that no upconverted fluorescence is visible upon excitation with a 635-nm laser diode. Nevertheless, these complexes act as efficient sensitizers upon excitation at shorter wavelength. Indeed, the upconverted fluorescence is observed upon excitation with 590-nm LED (Figure 7). Similarly, the red LEDs can be used to obtain the upconverted fluorescence in the case of the **Pt-1**-, **Pt-2**-, and **Pd-3**-based systems. We used the perylene bisimide

dx.doi.org/10.1021/ic301440k | Inorg. Chem. 2013, 52, 1206–1216

annihilator **per-2**, in combination with **Pd-3**, to generate yellow upconverted emission (see Figure 7).

Figure 8 shows the luminescence spectra for **Pd-2** and **Pt-2** (concentration of the sensitizers = 5×10^{-4} M), in the absence and the presence of the annihilator **per-1** (1×10^{-4} M). (Figure S12 in the Supporting Information shows similar spectra for **Pd-1** and **Pt-1**.) As can be seen, some residual phosphorescence of **Pt-1** is visible in the presence of the annihilator; however, for **Pd-1**, it is completely quenched, because of the longer luminescence decay times of the complex. A similar situation is observed for **Pd-2**, **Pd-3**, and **Pt-2**. The quantum yields of the upconverted fluorescence can be roughly estimated by comparison of the emission of the annihilator and the emission of the sensitizer in the absence of the annihilator. Of course, this is a very rough estimation, since a rather high concentration of sensitizer and annihilator is used, so aggregation of the dyes and the inner-filter effect should be considered. For deoxygenated solutions containing 1×10^{-4} M of a sensitizer and 5×10^{-4} M of **per-1** the quantum yields were estimated to be 2.0%, 1.6%, 6.2%, 2.0%, and 2.0% for **Pd-1**, **Pt-1**, **Pd-2**, **Pt-2**, and **Pd-3**, respectively. Note that due to the different excitation wavelength the intensity of the excitation light could not be kept constant and was 2.4×10^{20}, 2.1×10^{20}, 2.3×10^{20}, 1.9×10^{20}, and 1.8×10^{20} ph s^{-1} m^{-2} for the same respective sensitizers. As can be seen, despite their poor phosphorescence, the Pd(II) complexes are better sensitizers than the respective Pt(II) complexes, which can be explained by significantly longer decay time of the former. Interestingly, the Pd(II) and Pt(II) complexes with **2** appear to be the strongest sensitizers among the investigated dyes which again correlates well with the longer lifetimes of the triplet state. The Φ values can be higher if stronger excitation is used since these light intensities are below the saturation values. Notably, some nonemissive metal complexes (such as a Ru(II) complex-coumarin dyad) were also reported to be efficient sensitizers.[67] For comparison, a model system that relies on PtTPTBP as a sensitizer showed the upconversion quantum yield of 4.4% (λ_{exc} = 615 nm, photon flux density = 1.8×10^{20} ph s^{-1} m^{-2}).

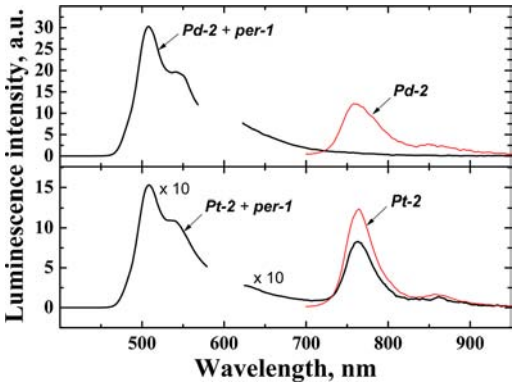

Figure 8. Emission spectra of 1×10^{-4} M deoxygenated toluene solutions of the sensitizer in the absence and the presence of 5×10^{-4} M of the annihilator **per-1** (thin red line and thick black lines, respectively). The excitation wavelengths were 586 and 600 nm for **Pd-2** and **Pt-2**, respectively, and the photon flux density values were 2.3×10^{20} and 1.9×10^{20} ph s^{-1} m^{-2}, respectively. Note that the emission slits at the fluorimeter were not identical for **Pd-2** and **Pt-2**.

Figure 9 shows the dependences of the intensity of the upconverted fluorescence on the photon flux density of the excitation light. As can be seen, all the sensitizers show a quadratic dependence at lower light intensities, which is typical for a nonlinear process such as TTA-based upconversion.[23,31,33,68] However, some deviation from the quadratic dependence is clearly visible in the case of **Pd-1** and **Pd-2** for photon flux densities exceeding 7×10^{19} ph s^{-1} m^{-2}. Indeed, at the light intensities significantly exceeding the threshold value, only a linear dependence of the upconverted fluorescence on the intensity of excitation light is observed.[20,69] The threshold intensities for the Pd(II) Schiff base complexes are expected to be slightly lower than those for the Pt(II) complexes, since the former proved to be better sensitizers of the upconverted fluorescence. It can be concluded here that the new Pt(II) and Pd(II) complexes represent a new class of efficient sensitizers of TTA upconversion and, therefore, may be promising for photovoltaic applications. Their broad absorption spectrum and high molar absorption coefficients are particularly attractive, since higher part of the solar spectrum can be collected compared to the state-of-the-art sensitizers such as metal complexes of benzoporphyrins. The same principle can be used to enable other potential applications such as imaging in scattering media and in tissues, which will require much lower excitation light intensities than, e.g., 2-photon microscopy.[70] In this case, the red-light excitability of the new sensitizers is important, because of deeper light penetration and lower light scattering. The new sensitizers can be also promising for application in anti-Stokes oxygen sensors, which also make use of TTA-based upconversion.[71]

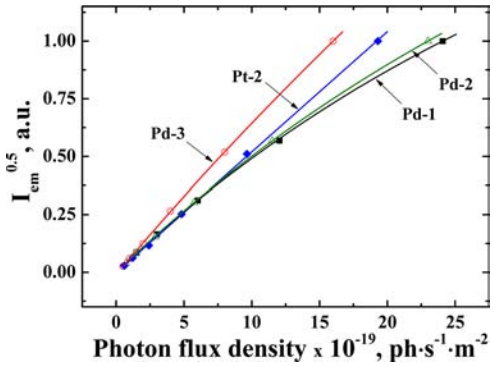

Figure 9. Effect of excitation intensity on the intensity of the upconverted fluorescence for the deoxygenated toluene solutions containing 1×10^{-4} M of the sensitizer and 5×10^{-4} M of **per-1**(λ_{exc} 583, 586, 600, and 607 nm for **Pd-1**, **Pd-2**, **Pt-2**, and **Pd-3**, respectively).

CONCLUSIONS

We have presented new phosphorescent dyes based on Pt(II) and Pd(II) complexes with donor–acceptor Schiff bases. The new dyes absorb in the red part of the spectrum and emit in the near infrared (NIR) region. The spectral properties can be tuned by varying the nature of the Schiff base. Pt(II) complexes belong to fairly strong emitters, but the respective Pd(II) complexes possess significantly lower luminescence brightness. The absorption and the emission bands of the ligands and the complexes shift bathochromically as the polarity of the solvent increases. Also, the luminescence quantum yields and the decay time decrease with increasing polarity. We have demonstrated that Pt(II) complexes can be used as indicators for optical sensing of oxygen where they may represent an alternative to the benzoporphyrin complexes. Both Pd(II) and Pt(II) complexes are efficient sensitizers of triplet–triplet annihila-

dx.doi.org/10.1021/ic301440k | Inorg. Chem. 2013, 52, 1206–1216

tion-based upconverted fluorescence. Particularly, because of the broad absorption bands and very high molar absorption coefficients they can collect significantly more light in the orange-red part of the spectrum than state-of-the-art sensitizers. The availability of the complexes via simple two-step synthesis from commercially available chemicals can be advantageous for practical applications. Lower photostability of the new dyes, compared to the Pt(II) tetraphenyltetrabenzoporphyrin, should be considered.

■ ASSOCIATED CONTENT

Supporting Information

X-ray crystallographic data for **Pd-3** in CIF format, ^{1}H and ^{13}C NMR, mass spectra of the ligands and complexes, excitation spectra and details on photobleaching experiments. This material is available free of charge via the Internet at http://pubs.acs.org.

■ AUTHOR INFORMATION

Corresponding Author

*Tel.: +43 316 873 32516. Fax: +43 316 873 32502. E-mail: sergey.borisov@tugraz.at.

Notes

The authors declare no competing financial interest.

■ ACKNOWLEDGMENTS

Financial support from the European Research Council (Project "Oxygen", No. 207233) is gratefully acknowledged.

■ REFERENCES

(1) Evans, R. C.; Douglas, P.; Winscom, C. J. *Coord. Chem. Rev.* **2006**, *250*, 2093−2126.
(2) Gareth Williams, J. A.; Develay, S.; Rochester, D. L.; Murphy, L. *Coord. Chem. Rev.* **2008**, *252*, 2596−2611.
(3) Xiao, L.; Chen, Z.; Qu, B.; Luo, J.; Kong, S.; Gong, Q.; Kido, J. *Adv. Mater.* **2011**, *23*, 926−952.
(4) Jung, I.; Choi, H.; Lee, J. K.; Song, K. H.; Kang, S. O.; Ko, J. *Inorg. Chim. Acta* **2007**, *360*, 3518−3524.
(5) Currie, M. J.; Mapel, J. K.; Heidel, T. D.; Goffri, S.; Baldo, M. A. *Science* **2008**, *321*, 226−228.
(6) Wolfbeis, O. S. *J. Mater. Chem.* **2005**, *15*, 2657−2669.
(7) Amao, Y.; Okura, I. *J. Porphyrins Phthalocyanines* **2009**, *13*, 1111−1122.
(8) Papkovsky, D. B.; O'Riordan, T. C. *J. Fluoresc.* **2005**, *15*, 569−584.
(9) Fernández-Moreira, V.; Thorp-Greenwood, F. L.; Coogan, M. P. *Chem. Commun.* **2009**, *46*, 186−202.
(10) Baggaley, E.; Weinstein, J. A.; Williams, J. A. G. *Coord. Chem. Rev.* **2012**, *256*, 1762−1785.
(11) Stein, E. W.; Grant, P. S.; Zhu, H.; McShane, M. J. *Anal. Chem.* **2007**, *79*, 1339−1348.
(12) Lebedev, A. Y.; Cheprakov, A. V.; Sakadžić, S.; Boas, D. A.; Wilson, D. F.; Vinogradov, S. A. *Appl. Mater. Interfaces* **2009**, *1*, 1292−1304.
(13) Yaseen, M. A.; Srinivasan, V. J.; Sakadzic, S.; Wu, W.; Ruvinskaya, S.; Vinogradov, S. A.; Boas, D. A. *Opt. Express.* **2009**, *17*, 22341−22350.
(14) Obata, M.; Hirohara, S.; Tanaka, R.; Kinoshita, I.; Ohkubo, K.; Fukuzumi, S.; Tanihara, M.; Yano, S. *J. Med. Chem.*. **2009**, *52*, 2747−2753.
(15) Sommer, J. R.; Farley, R. T.; Graham, K. R.; Yang, Y.; Reynolds, J. R.; Xue, J.; Schanze, K. S. *Appl. Mater. Interfaces* **2009**, *1*, 274−278.
(16) Borek, C.; Hanson, K.; Djurovich, P. I.; Thompson, M. E.; Aznavour, K.; Bau, R.; Sun, Y.; Forrest, S. R.; Brooks, J.; Michalski, L.; Brown, J. *Angew. Chem., Int. Ed.* **2007**, *46*, 1109−1112.
(17) Sun, Y.; Borek, C.; Hanson, K.; Djurovich, P. I.; Thompson, M. E.; Brooks, J.; Brown, J. J.; Forrest, S. R. *Appl. Phys. Lett.* **2007**, *90*, 213503.
(18) Singh-Rachford, T. N.; Castellano, F. N. *Coord. Chem. Rev.* **2010**, *254*, 2560−2573.
(19) Zhao, J.; Ji, S.; Guo, H. *RSC Adv.* **2011**, *1*, 937−950.
(20) Monguzzi, A.; Tubino, R.; Hoseinkhani, S.; Campione, M.; Meinardi, F. *Phys. Chem. Chem. Phys.* **2012**, *14*, 4322−4332.
(21) Hou, J.; Park, M.-H.; Zhang, S.; Yao, Y.; Chen, L.-M.; Li, J.-H.; Yang, Y. *Macromolecules* **2008**, *41*, 6012−6018.
(22) Islangulov, R. R.; Kozlov, D. V.; Castellano, F. N. *Chem. Commun.* **2005**, 3776−3778.
(23) Islangulov, R. R.; Lott, J.; Weder, C.; Castellano, F. N. *J. Am. Chem. Soc.* **2007**, *129*, 12652−12653.
(24) Ji, S.; Wu, W.; Wu, W.; Guo, H.; Zhao, J. *Angew. Chem., Int. Ed.* **2011**, *50*, 1626−1629.
(25) Wu, W.; Guo, H.; Wu, W.; Ji, S.; Zhao, J. *Inorg. Chem.* **2011**, *50*, 11446−11460.
(26) Sun, J.; Wu, W.; Zhao, J. *Chem.—Eur. J.* **2012**, *18*, 8100−8112.
(27) Wu, W.; Sun, J.; Ji, S.; Wu, W.; Zhao, J.; Guo, H. *Dalton Trans.* **2011**, *40*, 11550−11561.
(28) Wu, W.; Wu, W.; Ji, S.; Guo, H.; Zhao, J. *Dalton Trans.* **2011**, *40*, 5953−5963.
(29) Yi, X.; Zhao, J.; Wu, W.; Huang, D.; Ji, S.; Sun, J. *Dalton Trans.* **2012**, *41*, 8931−8940.
(30) Sun, J.; Wu, W.; Guo, H.; Zhao, J. *Eur. J. Inorg. Chem.* **2011**, *2011*, 3165−3173.
(31) Singh-Rachford, T. N.; Castellano, F. N. *J. Phys. Chem. A* **2008**, *112*, 3550−3556.
(32) Turshatov, A.; Busko, D.; Baluschev, S.; Miteva, T.; Landfester, K. *New J. Phys.* **2011**, *13*, 083035.
(33) Singh-Rachford, T. N.; Haefele, A.; Ziessel, R.; Castellano, F. N. *J. Am. Chem. Soc.* **2008**, *130*, 16164−16165.
(34) Singh-Rachford, T. N.; Castellano, F. N. *J. Phys. Chem. Lett.* **2010**, *1*, 195−200.
(35) Monguzzi, A.; Tubino, R.; Meinardi, F. *J. Phys. Chem. A* **2009**, *113*, 1171−1174.
(36) Baluschev, S.; Yakutkin, V.; Wegner, G.; Miteva, T.; Nelles, G.; Yasuda, A.; Chernov, S.; Aleshchenkov, S.; Cheprakov, A. *Appl. Phys. Lett.* **2007**, *90*, 181103-1−181103-3.
(37) Wu, W.; Guo, H.; Wu, W.; Ji, S.; Zhao, J. *J. Org. Chem.* **2011**, *76*, 7056−7064.
(38) Wu, W.; Zhao, J.; Guo, H.; Sun, J.; Ji, S.; Wang, Z. *Chem.—Eur. J.* **2012**, *18*, 1961−1968.
(39) Vinogradov, S. A.; Wilson, D. F. *J. Chem. Soc., Perkin Trans. 2.* **1995**, 103.
(40) Finikova, O. S.; Cheprakov, A. V.; Beletskaya, I. P.; Carroll, P. J.; Vinogradov, S. A. *J. Org. Chem.* **2004**, *69*, 522−535.
(41) Borisov, S. M.; Nuss, G.; Haas, W.; Saf, R.; Schmuck, M.; Klimant, I. *J. Photochem. Photobiol. A* **2009**, *201*, 128−135.
(42) Rozhkov, V. V.; Khajehpour, M.; Vinogradov, S. A. *Inorg. Chem.* **2003**, *42*, 4253−4255.
(43) Finikova, O. S.; Cheprakov, A. V.; Carroll, P. J.; Vinogradov, S. A. *J. Org. Chem.* **2003**, *68*, 7517−7520.
(44) Finikova, O. S.; Aleshchenkov, S. E.; Briñas, R. P.; Cheprakov, A. V.; Carroll, P. J.; Vinogradov, S. A. *J. Org. Chem.* **2005**, *70*, 4617−4628.
(45) Niedermair, F.; Borisov, S.; Zenkl, G.; Hotmann, O.; Weber, H.; Saf, R.; Klimant, I. *Inorg. Chem.* **2010**, *49*, 9333−9342.
(46) Rosenow, T. C.; Walzer, K.; Leo, K. *J. Appl. Phys.* **2008**, *103*, 043105.
(47) Borisov, S.; Zenkl, G.; Klimant, I. *ACS Appl. Mater. Interfaces* **2010**, *2*, 366−374.
(48) Borisov, S. M.; Papkovsky, D. B.; Ponomarev, G. V.; DeToma, A. S.; Saf, R.; Klimant, I. *J. Photochem. Photobiol. A.* **2009**, *206*, 87−92.
(49) Palmer, J. H.; Durrell, A. C.; Gross, Z.; Winkler, J. R.; Gray, H. B. *J. Am. Chem. Soc.* **2010**, *132*, 9230−9231.
(50) Che, C.-M.; Chan, S.-C.; Xiang, H.-F.; Chan, M. C. W.; Liu, Y.; Wang, Y. *Chem. Commun.* **2004**, 1484−1485.

(51) Che, C.-M.; Kwok, C.-C.; Lai, S.-W.; Rausch, A. F.; Finkenzeller, W. J.; Zhu, N.; Yersin, H. *Chem.—Eur. J.* **2010**, *16*, 233−247.
(52) Kanthimathi, M.; Dhathathreyan, A.; Nair, B. U. *Chem. Phys. Lett.* **2000**, *324*, 43−47.
(53) Wang, P.; Hong, Z.; Xie, Z.; Tong, S.; Wong, O.; Lee, C.; Wong, N.; Hung, L.; Lee, S. *Chem. Commun.* **2003**, 1664−1665.
(54) Hai, Y.; Chen, J.-J.; Zhao, P.; Lv, H.; Yu, Y.; Xu, P.; Zhang, J.-L. *Chem. Commun.* **2011**, *47*, 2435−2437.
(55) Tsatsaroni, E. G.; Lin, S. M.; Peters, A. T. *Coloration Technol.* **1999**, *115*, 62−68.
(56) Lacroix, P. G.; Di Bella, S.; Ledoux, I. *Chem. Mater.* **1996**, *8*, 541−545.
(57) Velapoldi, R. A.; Tønnesen, H. H. *J. Fluoresc.* **2004**, *14*, 465−472.
(58) Seybold, G.; Wagenblast, G. *Dyes Pigm.* **1989**, *11*, 303−317.
(59) SHELX and SHELXL PC: VERSION 5.03; Bruker AXS, Inc.: Madison, WI, 1994.
(60) SADABS: Area-detection Absorption Correction; Bruker AXS, Inc.: Madison, WI, 1995.
(61) Borisov, S. M.; Klimant, I. *Dyes Pigm.* **2009**, *83*, 312−316.
(62) Liu, X.; Cole, J. M.; Waddell, P. G.; Lin, T.-C.; Radia, J.; Zeidler, A. *J. Phys. Chem. A* **2012**, *116*, 727−737.
(63) Carraway, E. R.; Demas, J. N.; DeGraff, B. A.; Bacon, J. R. *Anal. Chem.* **1991**, *63*, 337−342.
(64) Finikova, O. S.; Lebedev, A. Y.; Aprelev, A.; Troxler, T.; Gao, F.; Garnacho, C.; Muro, S.; Hochstrasser, R. M.; Vinogradov, S. A. *ChemPhysChem.* **2008**, *9*, 1673−1679.
(65) Sakadzic, S.; Roussakis, E.; Yaseen, M. A.; Mandeville, E. T.; Srinivasan, V. J.; Arai, K.; Ruvinskaya, S.; Devor, A.; Lo, E. H.; Vinogradov, S. A.; Boas, D. A. *Nat. Meth.* **2010**, *7*, 755−759.
(66) Borisov, S. M.; Nuss, G.; Klimant, I. *Anal. Chem.* **2008**, *80*, 9435−9442.
(67) Ji, S.; Guo, H.; Wu, W.; Wu, W.; Zhao, J. *Angew. Chem., Int. Ed.* **2011**, *50*, 8283−8286.
(68) Singh-Rachford, T. N.; Lott, J.; Weder, C.; Castellano, F. N. *J. Am. Chem. Soc.* **2009**, *131*, 12007−12014.
(69) Monguzzi, A.; Mezyk, J.; Scotognella, F.; Tubino, R.; Meinardi, F. *Phys. Rev. B* **2008**, *78*, 195112.
(70) Wohnhaas, C.; Turshatov, A.; Mailänder, V.; Lorenz, S.; Baluschev, S.; Miteva, T.; Landfester, K. *Macromol. Biosci.* **2011**, *11*, 772−778.
(71) Borisov, S. M.; Larndorfer, C.; Klimant, I. *Adv. Funct. Mater.* **2012**, *22*, 4360−4368.